Energy 61 (2013) 447–454

Contents lists available at ScienceDirect

Energy

journal homepage: www.elsevier.com/locate/energy

# Vertically mounted bifacial photovoltaic modules: A global analysis

Siyu Guo [a, b, *], Timothy Michael Walsh [a], Marius Peters [a]

[a] Solar Energy Research Institute of Singapore, National University of Singapore, Singapore 117574, Singapore
[b] Electrical and Computer Engineering (ECE), NUS, Singapore 117576, Singapore

ARTICLE INFO

*Article history:*
Received 4 March 2013
Received in revised form
12 July 2013
Accepted 21 August 2013
Available online 23 September 2013

*Keywords:*
PV energy
Bifacial PV module
Mono-facial PV module
Diffuse fraction
Albedo

ABSTRACT

Bifacial PV (photovoltaic) modules have recently come to increasing attention and various system designs have been investigated. In this paper, a global comparison is made between vertically mounted bifacial modules facing East–West and conventionally mounted mono-facial modules. An analytical method is used to calculate the radiation received by these two module configurations. It is found that the answer to the question which of these two module configurations performs better strongly depends on three factors: (i) the latitude, (ii) the local diffuse fraction and (iii) the albedo. In a subsequent part of the paper, the minimum albedo required to result in a better performance for vertically mounted bifacial modules is calculated for every place in the world. The calculation is based on measured data of the diffuse light fraction and the results are shown in the form of a global map. Finally, the albedo requirements are compared with the measured global albedo distribution. The calculation allows a distinct decision which module configuration is more suitable for a certain place in the world. The result is also shown as a map defining the corresponding areas.



## 1. Introduction

The fast depleting of conventional energy sources and increasing energy demand are encouraging the development on PV (photovoltaic) technologies [1]. Among different kinds of PV technologies, interest in bifacial PV modules is increasing in recent years [2,3]. There are several reasons for this. Glass–glass PV module construction technology seems to have more benefits in terms of durability compared to glass-backsheet module construction [4]. Advanced solar cell manufacturing methods such as ion-implantation and heterojunction technologies not only result in high efficiency solar cells, but also naturally result in bifacial solar cells, unlike the aluminium back surface field solar cells which dominate the PV (photovoltaic) market today [5–8]. The structures of mono-facial and bifacial p-type substrate crystalline silicon solar cells are shown as an example in Fig. 1. The local contact on the back surface of bifacial solar cells allows them to absorb light from both the front side and the back side. Their corresponding module structures are also included in Fig. 1. Instead of having backsheet on the back of mono-facial PV modules, bifacial modules have glass on their back side which allows them to make use of the light coming from both sides. Depending on the installation, bifacial modules can produce up to 20% more energy in side-by-side comparisons than equivalent mono-facial modules [9], and the cost of a bifacial PV module is equal to the cost of a conventional mono-facial module with the same front surface [10]. Bifacial modules can be installed vertically facing (East–West), which, depending on the application, can save space, and depending on several factors, can, in this orientation, produce as much energy per Watt as conventionally mounted mono-facial PV modules (tilted at latitude towards the equator) [11,12]. The generation profile of such a vertically mounted bifacial PV module is significantly different to that of a conventionally mounted mono-facial module (see Fig. 3). The VMBM (vertically mounted bifacial module) facing East–West produces more energy in the early morning and late afternoon than CMMM (conventionally mounted mono-facial modules). With increasing penetration of PV electricity generation in a grid (e.g. in Germany), this rare double-humped “bactrian camel” of Central Asia, is far more valuable than the single-humped “dromedary camel” of Arabia. VMBMs also have further advantages. They can, for example, be installed as sound barriers along roadsides and they are less prone to be covered by snow. For these reasons it is necessary to investigate how the performance of VMBM is affected by the environmental factors and how it compares with CMMM.

In this paper, MATLAB-based simulation is used to investigate factors affecting and influencing the amount of energy which can be produced by a VMBM. Also, a global comparison is made

* Corresponding author. 7 Engineering Drive 1, Blk E3A #06-1, Singapore 117574, Singapore. Tel.: +65 84816719.
*E-mail address:* guo_siyu@nus.edu.sg (S. Guo).

0360-5442/$ – see front matter © 2013 Elsevier Ltd. All rights reserved.
http://dx.doi.org/10.1016/j.energy.2013.08.040

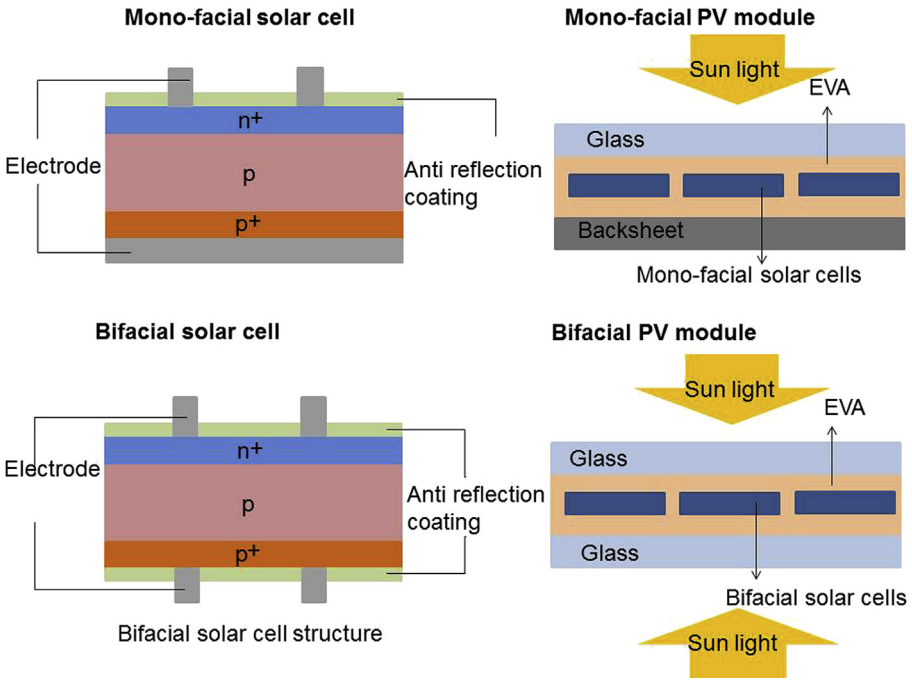


**Fig. 1.** Structure of mono-facial solar cells (upper left), mono-facial PV modules (upper right), bifacial solar cells (lower left) and bifacial PV modules (lower right).

between VMBM and CMMM in order to evaluate which kind of PV module is more suitable for a certain location. The setups of the two modules are shown in Fig. 2. It is found that the performance of a bifacial module strongly depends on latitude, diffuse fraction and albedo, and the difference between the performances of VMBM and CMMM also strongly depends on these factors. Based on measured diffuse light fraction data, the minimum albedo required so that a VMBM performs better than a CMMM is calculated for every place in the world. The calculation is based on the annually received radiation and is therefore not specific to any kind of solar cell.

## 2. Theory and method

### 2.1. Simulation of direct and diffuse radiation

The method introduced in this part is used to calculate the radiation received by a PV module at a certain place in the world during a whole year for a certain fraction of diffuse light. The radiation received by a module can be divided into two parts: diffuse radiation and direct radiation. Each part is related to a certain fraction of radiation called diffuse and direct fraction. In this part, the direct and diffuse radiation is simulated under a certain transmittance coefficient $\tau$.

In the first step, the extraterrestrial radiation, which describes the intensity of solar radiation directly outside the earth's atmosphere on a horizontal surface, is calculated with a yearly varying term [13]:

$$I_0 = 1367.7 \times \left[1 + 0.033 \times \cos\left(\frac{2\pi}{365} \times \mathrm{DOY}\right)\right] \quad (1)$$

$I_0$: extraterrestrial radiation; DOY: day of a year, DOY = 1 if the date is January 1st.

Direct normal radiation, which is defined as the solar radiation incident on a surface oriented normal to the solar radiation, can be calculated from the exterritorial radiation, which is a function of the transmission coefficient [14]. This relationship is based on a model developed by Liu and Jordan [15]. In this model, DNI (direct normal incidence) is calculated as a function of AM (air mass). Air mass is the path length which light takes through the atmosphere normalised to the shortest possible path length, which is described as:

$$\mathrm{AM} = \frac{1}{\cos(\theta)} \quad (2)$$

$\theta$: zenith angle of the sun.

With a known air mass value, the direct normal incidence is calculated by:

$$\mathrm{DNI} = I_0 \times \tau^{\mathrm{AM}} \quad (3)$$

DNI: direct normal incidence; AM: air mass; $\tau$: transmission coefficient for direct solar radiation.

If DNI is known, horizontal direct radiation ($H_{\mathrm{dir}}$), which refers to the direct radiation incidents on a horizontal surface, can be calculated directly from:

$$H_{\mathrm{dir}} = \mathrm{DNI} \times \cos(\theta) \quad (4)$$

In the next step, horizontal diffuse radiation ($H_{\mathrm{diff}}$), which is defined as the amount of diffuse radiation incidents on a horizontal surface, needs to be calculated. Campbell and Norman developed a relationship between horizontal diffuse radiation and transmission coefficient based on Liu and Jordan's model, which is described by Ref. [16]:

$$H_{\mathrm{diff}} = 0.3\left(1 - \tau^{\mathrm{AM}}\right) I_0 \cos(\theta) \quad (5)$$

However, this model is mostly used to model clear-sky condition when the transmission coefficient $\tau$ is larger than 0.45 and might not be very suitable for overcast conditions. Under overcast conditions, there are no existing models that directly relate diffuse radiation to the transmittance coefficient $\tau$. However, there are many models that relate diffuse fraction $k_{\mathrm{d}}$ to clearness index $k_{\mathrm{t}}$. Clearness index $k_{\mathrm{t}}$ can be used to generate synthetic solar radiation data and estimate the PV system performance [17]. The models that

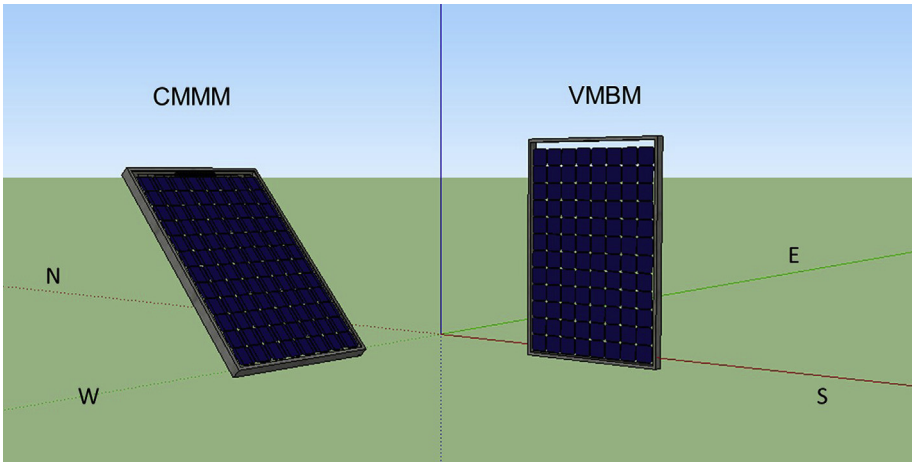


**Fig. 2.** The setups of a VMBM and a CMMM. VMBM represents a vertically mounted bifacial module facing East–West, and CMMM represents a conventionally mounted mono-facial module. The CMMM shown in the figure is in the north hemisphere, and the tilting angle of the CMMM $\omega$ is equal to the latitude of its location.

relate $k_d$ to $k_t$ have been analysed and evaluated in Ref. [18]. Diffuse radiation can be related to the transmittance coefficient by this kind of relationship, and this relationship was used before to optimise solar energy extraction under cloudy conditions [19]. Here,

$$k_d = \frac{H_{diff}}{H_{dir} + H_{diff}} \tag{6}$$

$$k_t = \frac{H_{dir} + H_{diff}}{I_0 \times \cos\theta} \tag{7}$$

$$k_b = \frac{H_{dir}}{I_0 \times \cos\theta} \tag{8}$$

The global radiation on both bright and overcast conditions is split into its direct beam and diffuses components using a diffuse fraction correlation $k_d$. The expression estimates the diffuse fraction as a function of the clearness index, $k_t$, and the general expression is described as follows:

$$k_d = A + Bk_t \tag{9}$$

since

$$k_d \times k_t + k_b = k_t \tag{10}$$

$k_b$ can be calculated from (7), and $k_t$ and $k_d$ can be calculated using (8) and (9):

$$k_t = -\frac{(A-1) + \sqrt{(A-1)^2 - 4B}}{2B} \tag{11}$$

$$k_d = -\frac{(A+1) - \sqrt{(A-1)^2 - 4B}}{2} \tag{12}$$

In this work, different models describing the relationship between $k_t$ and $k_d$ are used for calculation in order to verify the model. A review of different models can be found in Ref. [20]. The description of different models used in this work is shown in Table 1.with $k_t$ and $k_d$, horizontal diffuse radiation can be calculated by:

$$H_{diff} = I_0 \cos(\theta) \times k_t \times k_d \tag{13}$$

At last, the average diffuse fraction for one year can be calculated from:

$$\text{diffuse fraction} = \frac{H_{diff}(\text{for one year})}{H_{diff}\ (\text{for one year}) + H_{dir}(\text{for one year})} \tag{14}$$

In the calculation, an average annual transmittance coefficient is assumed. By changing this coefficient from 0 to 1, total $H_{diff}$ and $H_{dir}$ is integrated over the time of a year, and the average diffuse fraction can be calculated corresponding to certain average transmittance coefficient from Equation (13). After that, radiation received by a bifacial/mono-facial module for a year can be calculated under different average diffuse fraction. In the next part, the method of calculating radiation received by a tilted surface will be introduced.

### 2.2. Simulation of radiation received by a tilted surface

In order to calculate the radiation received by both bifacial and mono-facial PV modules, a method to calculate radiation received by a tilted surface is described in this part. Similar methods that help simulate radiation received by bifacial modules can be found in Refs. [23,24]. These methods can also be used to model the radiation received by PV modules with solar-tracking systems [25,26].

The sun's position can be described by two angles: azimuth and altitude. These two angles of the sun during a whole year for any places in the world can be calculated by existing models [13]. The configuration of a PV module can also be described by two angles: tilting angle and azimuth.

Assuming $\beta_{sun}$ is the altitude angle and $\alpha_{sun}$ is the azimuth angle of the solar position, $\omega$ is the tilting angle of the module, $\alpha$ is the difference between the sun's and the module's azimuth angles: $\alpha = \alpha_{sun} - \alpha_{module}$, the solar incidence angle $\gamma$ is the angle between the normal of the module and the sun's rays, the amount of direct-beam solar radiation received by a tilted surface ($S_{dir}$) is calculated by:

$$S_{dir} = \text{DNI} \times \cos(\gamma) \tag{15}$$

**Table 1**
Description of different models used in calculation relating $k_t$ and $k_d$.

| Model | $A$ | $B$ | Range |
|---|---|---|---|
| Reindl et al. [21] | 1.02 | −0.248 | $k_t \le 0.3$ |
| | 1.45 | −1.67 | $0.3 < k_t < 0.78$ |
| | 0.147 | 0 | $k_t \ge 0.78$ |
| Orgill and Hollands [22] | 1 | −0.249 | $k_t < 0.35$ |
| | 1.577 | −1.84 | $0.35 \le k_t \le 0.75$ |
| | 0.177 | 0 | $k_t > 0.75$ |

The angle between two vectors in a three dimensional space is calculated by:

$$\cos(\gamma) = \boldsymbol{a} \times \boldsymbol{b}/(|\boldsymbol{a}| \times |\boldsymbol{b}|) \tag{16}$$

Thus the direct radiation received by a module's front side is calculated by:

$$S_{\text{direct}}(\text{front}) = \text{DNI} \times \frac{-\cos(\alpha)\sin(\omega) + \cos(\omega) \times \tan(\beta_{\text{sun}})}{\sqrt{1 + \tan^2(\beta_{\text{sun}})}} \tag{17}$$

Similarly, the direct radiation received by a module's back side is calculated by:

$$S_{\text{direct}}(\text{back}) = \text{DNI} \times \frac{\cos(\alpha)\sin(\omega) - \cos(\omega) \times \tan(\beta_{\text{sun}})}{\sqrt{1 + \tan^2(\beta_{\text{sun}})}} \tag{18}$$

Here, if the calculated radiation value is negative, the radiation received by that side is zero. At a certain time of a day, only one side of a PV module can receive direct radiation.

In practice, reflection also has an influence on the radiation received by a tilted surface, which also needs to be taken into account. The reflection loss ($R_{\text{loss}}$) for the direct beam incidents to a tilted surface is a function of the incident angle $\gamma$ [27]:

$$R_{\text{loss}}(\gamma) = 1 - \left[\frac{1 - \exp(-\cos\gamma/\text{ar})}{1 - \exp(-1/\text{ar})}\right] \tag{19}$$

ar is the angular loss coefficient. Typical ar values range from 0.16 to 0.17 for commercial crystalline silicon wafer modules [27].

In the next step, radiation reflected from the sky and radiation reflected from the ground seen by a tilted surface needs to be calculated, and a model by Tian et al. is used [28]. Diffuse radiation from the sky seen by a tilted surface is calculated by:

$$R_s = H_{\text{diff}} \times \text{svf} \tag{20}$$

Here, svf is sky-view factor which is calculated by:

$$\text{svf} = (\pi - \omega)/\pi; \quad \text{gvf} = 1 - \text{svf} \tag{21}$$

Radiation reflected from the ground seen by a tilted surface is calculated by Ref. [23]:

$$R_g = A \times \left(H_{\text{dir}} + H_{\text{diff}}\right) \times \text{gvf} \tag{22}$$

Here, $A$ is albedo of the ground and gvf is ground-view factor which is calculated by:

$$\text{gvf} = 1 - \text{svf} \tag{23}$$

At last, the total radiation received by a tilt surface ($S_{\text{total}}$) can be calculated based on Equations (15) and (24):

$$S_{\text{total}} = S_{\text{dir}} + H_{\text{diff}} \times \text{svf} + \text{A} \times \left(H_{\text{dir}} + H_{\text{diff}}\right) \times \text{gvf} - R_{\text{loss}} \tag{24}$$

## 3. Results and discussion

### 3.1. Daily radiation received by a bifacial module and a mono-facial module

From the calculation method described in Part 2, the total radiation received by a PV module with any configuration during a certain period can be calculated. As an example, Fig. 3 shows the simulated radiation received by a VMBM and a CMMM during a certain day in Singapore. Here, the mono-facial module is tilting at an angle which is equal to the latitude and facing the equator, and the bifacial module is tilting vertically facing east-west.

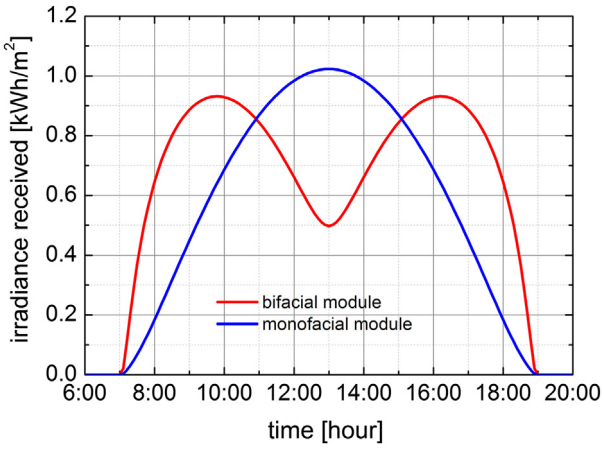


**Fig. 3.** Simulated radiation received by a VMBM and a CMMM on a certain day in Singapore. The diffuse fraction is set to be 0.18, and albedo is set to be 0.35, which are practical values for clear-sky conditions in Singapore. From the two curves, it is calculated that the radiation received by the VMBM in the whole day is 8.54 kWh, which is larger than the radiation received by the CMMM 7.38 kWh.

From Fig. 3 it can be observed that for a VMBM, there are two peaks on the daily radiation receive. One peak appears in the morning, and the other peak appears in the afternoon. This is due to the two situations in which the bifacial module receives most light. Curves like these are well known and have been shown for bifacial modules in different locations [2,12].

### 3.2. Relation between diffuse fraction and radiation received

For bifacial modules, tilting at 90° facing East–West (VMBM) is the most commonly used configuration, since this configuration is easy to be realised and also allows a relatively high performance for the modules. For mono-facial modules, many investigations have been done to find the angle that results in maximum energy output over a long period of time [17,29–31], and it is found that a mono-facial module will generate the maximum output when it tilts at an angle which is almost equal to the latitude and faces the equator (CMMM) [32–34]. In order to compare VMBM with CMMM, radiation received by these two kinds of modules is calculated as a function of diffuse fraction. Fig. 4(a) shows the radiation received by a CMMM facing the equator and a VMBM for a whole year in (a) Singapore (1° N) and (b) Berlin (52° N). The results are calculated based on the method described in Part 2. Today's bifacial and mono-facial modules have nearly the same single side efficiency. Furthermore, the efficiency for a bifacial module is almost equal, no matter from which side it is illuminated. Using these assumptions, we have calculated the energy output of the two modules, using a module efficiency of 16% in all cases. As the energy output of the two modules is proportional to the radiation they received, the calculated output power follows the same trend as the received illumination. The yearly energy output of each kind of module is calculated in Fig. 4(b). Here we just take the efficiency of PV modules made with crystalline silicon solar cells as an example. Since our analysis is quite general and not specific to a kind of solar cell, the energy output of any kinds of bifacial solar cells can be obtained by multiply the incoming power with the conversion efficiency.

From Fig. 4, it can be observed that for a low diffuse fraction, the radiation received by the VMBM is less than the radiation received

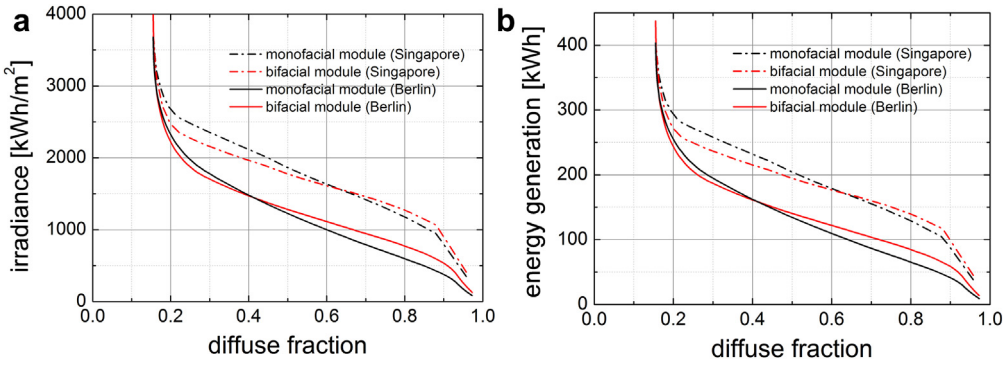


**Fig. 4.** (a) Radiation received and (b) energy generation by a CMMM and a VMBM calculated for a period of one year under different diffuse fractions in (a) Singapore (1° N) and (b) Berlin (52° N). The albedo is set to be 0.2 for both cases. Both the efficiencies of the bifacial module and the mono-facial modules are assumed to be 16%, which is a practical value for both types of modules made with crystalline silicon solar cells. The bifaciality of the bifacial module is assumed to be one.

by the CMMM for both places (Berlin and Singapore). This is because the VMBM receives less direct radiation than the CMMM. As the diffuse fraction increases, the amount of radiation received by the VMBM increases and for a certain diffuse fraction exceeds the amount of radiation received by the CMMM. The reason for this is that mono-facial modules only accept diffuse light on one side. In contrast, bifacial modules accept diffuse light on both sides and have, therefore, an advantage in making use of this radiation. Consequently, there must be an intersection of the two curves, which marks the diffuse fraction required so that VMBM and CMMM receive the same amount of radiation and generate the same amount of energy through one year. Comparing the curves for different places, it can be observed that the diffuse fraction that results in equal radiation received by a VMBM and a CMMM is specific to the latitude. The reason is that the tilt angle for CMMM in Singapore is close to zero degree, which is much smaller than the tilt angle for CMMM in Berlin (52°). Since the back surface of the mono-facial modules cannot receive diffuse light, a CMMM in Singapore receives almost 100% of the total diffuse light from the sky and nearly no diffuse light from the ground. However, a CMMM in Germany can only receive about 71% diffuse light from the sky and 29% diffuse light from the ground. Since under normal condition, diffuse light from the sky carries much more intensity than diffuse light from the ground, a CMMM in Singapore receives a much larger fraction of diffuse light than a CMMM in Berlin. Consequently, a higher diffuse fraction is needed to have a VMBM in Singapore receive an equal amount of radiation as a CMMM.

As mentioned, the diffuse fraction corresponding to the crossing point of the two curves defined in Fig. 4 is a function of latitude. Since we assume that bifacial modules and mono-facial modules have the same converting efficiency and the bifaciality of the module is 1, if this relation can be calculated, it can provide an overview of how much diffuse fraction is needed for a certain place to make the output of a VMBM equal to a CMMM. If the real diffuse fraction of that place is equal or larger than this value, VMBM is preferred. On the other hand, if the actual diffuse fraction is lower than this value, it is better to use VMBM.

Given this, we can calculate the fraction of diffuse light for which the two module configurations result in the same amount of light for each latitude. The result of this calculation is shown in Fig. 5. For numerical reasons, calculating the exact intersection point (as shown in Fig. 4) can be difficult. The result shown in Fig. 4 gives the condition for which a VMBM receives 1% radiation more than a CMMM. In order to verify the results, three different meteorological models to calculate the horizontal diffuse radiation under certain transmittance coefficient are used for comparison (shown in Fig. 5). Among these models, Compbell and Norman's model is shown in Equation (5), which is more suitable for clear-sky condition. Rendl's model and Ogill's model are described in Table 1, which are suitable for both clear-sky and overcast condition. It is observed that the curves obtained from different models agree quite well. This is reasonable, since no matter what kind of model is used, the difference of radiation received by the two kinds of modules only depends on the diffuse fraction. Their absolute values may change, but the crossing point of the two lines is only a function of diffuse fraction and doesn't change much. In Fig. 5, a constant albedo value of 0.2 is assumed and the real diffuse fraction data of some cities in the world are included. The data are obtained from NASA surface meteorology and solar energy: global data sets [35]. If a city is above the curve, the VMBM performs better than the CMMM in that city and vice versa.

As mentioned, the albedo used for Fig. 5 was 0.2. In reality, the albedo for different places is different. Since Albedo is the fraction of the radiation reflected from the ground into space, it has an influence on the curve shown in Fig. 5. Therefore, the same calculation as shown in Fig. 5 has been repeated for different albedo values. The results are shown in Fig. 6. From Fig. 6 it can be seen that as the albedo increases, a smaller diffuse fraction is required to make the VMBM and CMMM receive the same amount of radiation, and more cities move above the line. The reason is that as albedo increase, there is more diffuse light coming from the ground, and

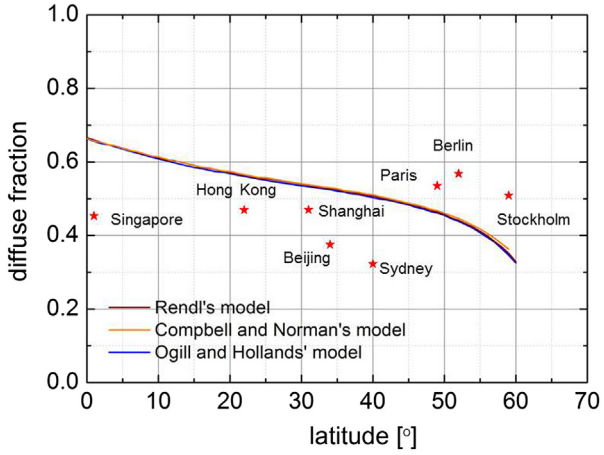


**Fig. 5.** Calculated diffuse fraction for which a VMBM receives 1% more radiation than a CMMM. The calculations were performed using three different meteorological models. The albedo of the ground is set to 0.2 here. If the actual diffuse fraction of a certain place is above the line, it is preferable to use VMBM instead of CMMM. Also given are the actual diffuse fractions for some cities [35].

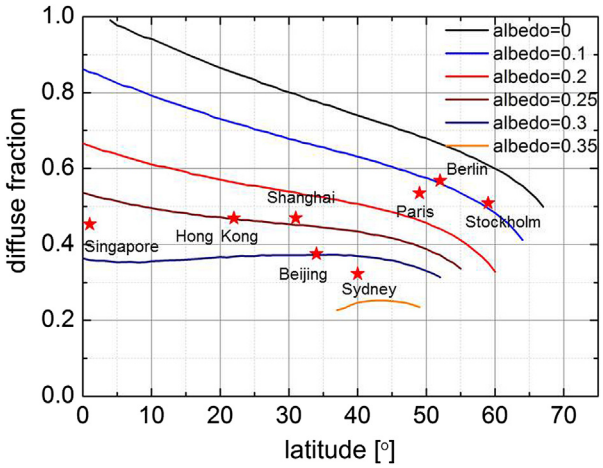


**Fig. 6.** Diffuse fraction for which a VMBM receives 1% more radiation than a CMMM, calculated as a function of latitude and for different albedo values. The stars in the figure indicate data for actual cities (compare Fig. 4).

the bifacial module can receive more diffuse light from the ground than the mono-facial module. When albedo increases to more than 0.35, the diffuse fraction that makes a VMBM receives 1% more radiation than a CMMM does not exist for a large range of latitudes. This means that for these places, even if the diffuse fraction reaches the minimum value, which is the minimum value that diffuse fraction can reach for a very-clear sky, a VMBM can still perform better than a CMMM. The reason is that the tilt angle for a CMMM, which is equal to the latitude, is small for low-latitude places. Thus the CMMM can receive only a small fraction of diffuse radiation from the ground. However, bifacial modules can receive all diffuse radiation from the ground. As the albedo value increases, diffuse radiation from the ground also increases, thus bifacial modules are more apt to receive more radiation for these places. When albedo reaches a certain value, even a very low diffuse fraction can still results in better performance for VMBM in these places.

### 3.3. A global comparison of VMBM and CMMM

Finally, we want to answer the following question: if the diffuse fraction of a certain place is already known, what is the minimum albedo value needed to make the VMBM perform better than the CMMM at this place? In order to solve this problem, the albedo value makes a VMBM receives 1% radiation more than a CMMM is calculated based on the actual diffuse fraction data of every place in the world. The data are again obtained from NASA surface meteorology and solar energy: global data sets [35]. The results are shown in Fig. 7. If the albedo of a place is larger than this value, the VMBM of that place performs better than the CMMM. Subsequently, the average albedo data for one year is calculated from the data set: ISLSCP II MODIS (Collection 4) Albedo, 2002 [36]. By comparing the calculated albedo value that results in a better performance of VMBM with the actual average albedo value, a decision can be made whether VMBM or CMMM is more suitable for a certain place in the world. The results are shown in Fig. 8.

From Fig. 8, for a large part of the high latitude places in the northern hemisphere, including Russia, Canada, Greenland and North and Central Europe, VMBMs show a very good performance and this configuration is preferable to CMMMs. The main reason is that only a small albedo value (less than 0.2) is required to result in a better performance of VMBM in these places, and the real albedo value is relatively high. For places like North Africa and Middle East, the albedo needed to have a VMBM perform better than a CMMM is relatively high; however, the real albedo value is higher. Thus for these places, it is also better to use VMBMs instead of CMMMs. In places like the United States, South America, Central and South Africa, India, East and South Asia and Australia, albedo values above 0.3 are needed to make a VMBM performs better. Since the real albedo value for these places is lower than the required values, CMMMs are favourable in these places. It should be noted that, since the data used in this work are obtained from satellite pictures, the results should be applied to large-scale PV power plants in countryside. In urban area, because of the surrounding buildings and some other factors, the diffuse fraction and albedo might be

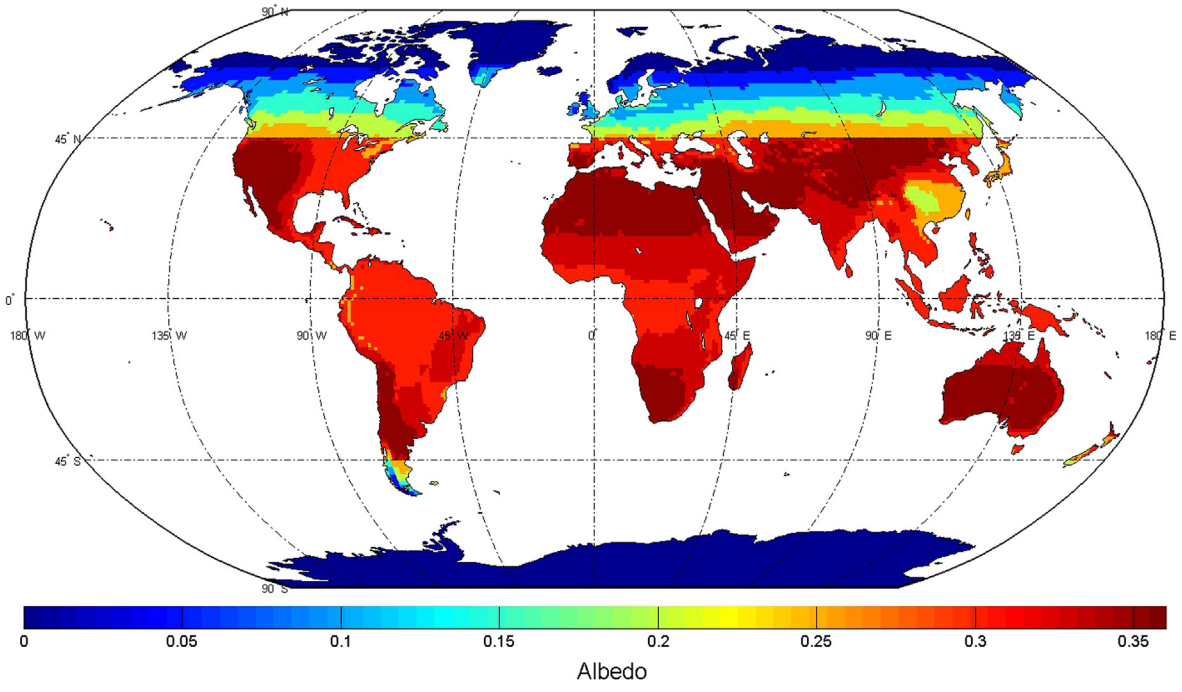


**Fig. 7.** The minimum albedo value corresponding to each place in the world above which the performance of a VMBM is better than the performance of a CMMM there.

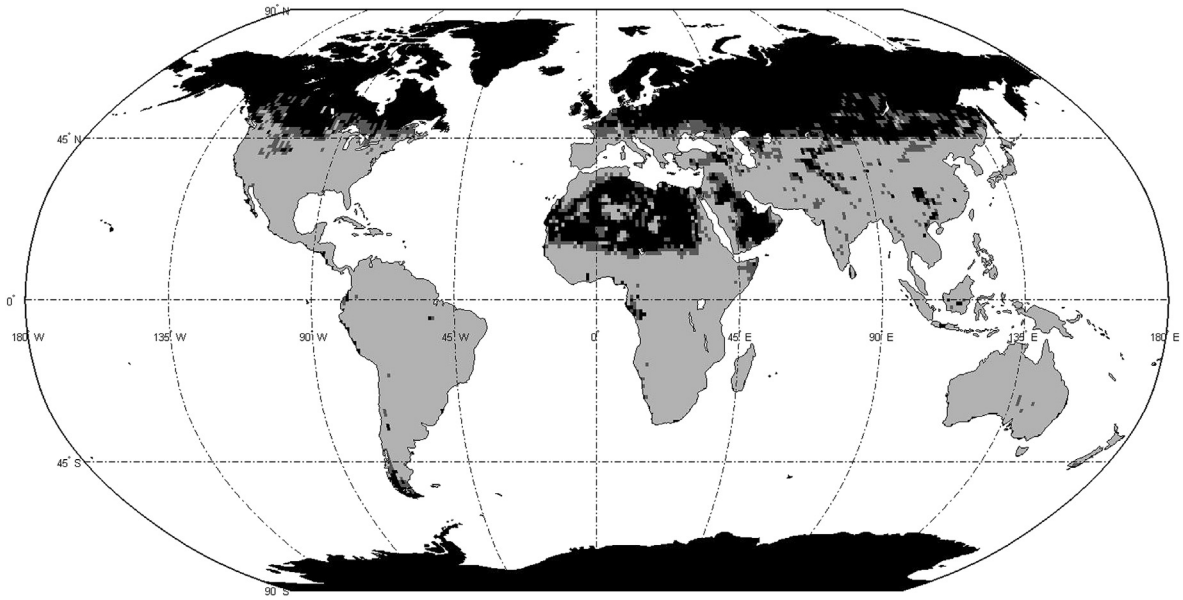


**Fig. 8.** Global map that representing which kind of module configuration results in better performance in a certain place. Black: VMBM. Light grey: CMMM. Dark grey: the two kinds of modules have very similar performance.

very different from the data obtained from the satellite picture. The method introduced in this paper is still valid for urban areas, but it must be analysed case-by-case based on the real albedo and diffuse fraction data of the specific location where PV modules are installed.

## 4. Error analysis

In this work, satellite-derived global irradiance data set and albedo data set are used as input in the calculation. Though satellite-derived data are generally less accurate than ground-measured data, they are available over large-areas and are suitable for global analysis. The inaccuracy of the result obtained from this work mainly comes from the inaccuracy of the two data sets: NASA surface meteorology and solar energy: global data sets and ISLSCP II MODIS (Collection 4) Albedo, 2002. An error analysis is done in this part in order to evaluate the validation of the result in this work.

For the NASA surface meteorology and solar energy: global data sets, the rRMSE (relative root mean square error) of the data is provided in Ref. [37]. The information is shown in Table 2.

Since the diffuse fraction is calculated by:

$$F_{\mathrm{diff}} = \frac{H_{\mathrm{diff}}}{H_{\mathrm{horiz}}} \tag{25}$$

According to the error propagation role, the rRMSE for diffuse fraction can be calculated as:

$$\frac{\delta F_{\mathrm{diff}}}{F_{\mathrm{diff}}} = \sqrt{\left(\frac{\delta H_{\mathrm{diff}}}{H_{\mathrm{diff}}}\right)^2 + \left(\frac{\delta H_{\mathrm{horiz}}}{H_{\mathrm{horiz}}}\right)^2} = 31.08\% \tag{26}$$

Since there is no direct relation between diffuse fraction and minimum albedo needed to result in a better performance of VMBM (Fig. 6) and the relationship is different for different latitude, we took the relationship for several different latitudes (from 5° to 70°) and made a polynomial fitting. After 70°, VMBM will always give a better performance no matter what the albedo value is.

According to the error propagation rule, if $y$ and $x$ have a relation $y = f(x)$, with a known relative error ($\delta x/x$) of parameter $x$, the relative error of $y$ can be calculated from:

$$\frac{\delta y}{y} = \sqrt{\left[\left(\frac{\partial y}{\partial x}\right)\delta x\right]^2} \tag{27}$$

By using this rule, the rRMSE was calculated for different latitudes. The maximum rRMSE we obtained is 25.19%, and the minimum rRMSE is 10.98%. As a result, the results obtained in Fig. 7 have a maximum rRMSE of 25.19%.

In the last part of section 3.3, the global albedo data set is used for deciding which kind of module configuration results in better performance in a certain place. For the data set ISLSCP II MODIS (Collection 4) Albedo, the accuracy is analysed in Refs. [38,39]. The accuracy of the data varies a little with different regions and the general rRMSE is within 6%.

As a consequence, using the data set from NASA surface meteorology and solar energy as input in or calculation, the maximum rRMSE is about 25.68%. The error of the results mainly comes from this input data set. If the ground-measured irradiance data can be used as input, the rRMSE of the result can be controlled within 10%.

## 5. Summary & conclusions

In this work, an analytical method was used to compare the radiation received by a VMBM (vertically mounted bifacial module) and a CMMM (conventionally mounted mono-facial module). It was found that the answer to the question, which of those module configurations performs better depends mainly on three factors: the latitude, the diffuse fraction and the albedo. With the method

**Table 2**
The accuracy of the horizontal insolation and horizontal diffuse radiation data used in the simulation of this work.

| Parameter | Region | rRMSE (%) |
|---|---|---|
| Horizontal insolation | Global | 10.25 |
| Horizontal diffuse radiation | Global | 29.34 |

developed here, it is possible to help choose a suitable module type for every place in the world.

At first, the method of calculating the diffuse fraction based on the transmittance coefficient was introduced, and the method of calculating the radiation received by a tilted surface is described. In the next step, the relation between diffuse fraction and radiation received by a module was investigated, and the diffuse fraction required to result in a better performance of the VMBM was calculated as a function of latitude. For this calculation different meteorological models have been used. It was found that the calculated required diffuse fraction agrees well for all used models. Finally, the minimum albedo value required to make a VMBM perform better than a CMMM is calculated based on real-measured diffuse fraction data for every place in the world. Comparing the required albedo with the real albedo distribution, the question that which module configuration performs better can be answered for every place in the world. Different regions in the world are analysed based on these results.

From the economic point of view, since the cost of the two kinds of modules is almost the same (there are no principle differences in the production of mono-facial and bifacial modules), we assume that the return of investment for these two kinds of modules only depends on the total radiation they received during their whole lifetime. This assumption is reasonable based on the data from today's PV industry [10]. As a result, Fig. 8 is also a figure that shows which kind of module has better performance from the economic point of view.

For these calculations we have made certain idealised assumptions. It is, for example assumed that the different modules have the same converting efficiency and that the bifaciality of the bifacial module is equal to one. Future steps will also take these factors into consideration and the developed method will be extended.

In conclusion, influence from latitude, diffuse fraction and albedo on two PV module configurations were investigated in this work. This investigation provides an overview of which of these configurations generates more output in a certain place.

## Acknowledgement

The Solar Energy Research Institute of Singapore (SERIS) is sponsored by the National University of Singapore (NUS) and Singapore's National Research Foundation (NRF) through the Singapore Economic Development Board (EDB). The diffuse fraction and albedo distribution data were obtained from the NASA Langley Research Center Atmospheric Science Data Center Surface meteorological and Solar Energy (SSE) web portal supported by the NASA LaRC POWER Project.

## References

[1] Singh GK. Solar power generation by PV (photovoltaic) technology: a review. Energy 2013;53:1–13.
[2] Uematsu T, Tsutsui K, Yazawa Y, Warabisako T, Araki I, Eguchi Y, et al. Development of bifacial PV cells for new applications of flat-plate modules. Sol Energ Mat Sol C 2003;75(3–4):557–66.
[3] bifi PV workshop. 2012http://bifipv-workshop.com/index.php?id=bifipv-start; 2013.
[4] Jorgensen GJ, Terwilliger KM, Kempe MD, McMahon TJ. Testing of packaging materials for improved PV module reliability. In: IEEE Phot Spec Conf 2005. p. 499–502.
[5] Ok YW, Upadhyaya AD, Tao YG, Zimbardi F, Ning S, Rohatgi A. Ion-implanted and screen-printed large area 19.6% efficient N-type bifacial Si solar cell. In: 2012 38th IEEE photovoltaic Specialists Conference (Pvsc) 2012. p. 2240–3.
[6] Eguren J, Delalamo J, Luque A. Optimization of P+ doping level of N+-P-P+ bifacial Bsf solar-cells by ion-implantation. Electron Lett 1980;16(16):633–4.
[7] Voz C, Munoz D, Fonrodona M, Martin I, Puigdollers J, Alcubilla R, et al. Bifacial heterojunction silicon solar cells by hot-wire CVD with open-circuit voltages exceeding 600 mV. Thin Solid Films 2006;511:415–9.
[8] Zhao L, Zhou CL, Li HL, Diao HW, Wang WJ. Design optimization of bifacial HIT solar cells on p-type silicon substrates by simulation. Sol Energy Mat Sol C 2008;92(6):673–81.
[9] Joge T, Eguchi Y, Imazu Y, Araki I, Uematsu T, Matsukuma K. Applications and field tests of bifacial solar modules. In: Conference Record of the Twenty-Ninth IEEE Photovoltaic Specialists Conference 2002 2002. p. 1549–52.
[10] Robles-Ocampo B, Ruiz-Vasquez E, Canseco-Sanchez H, Cornejo-Meza RC, Trapaga-Martinez G, Garcia-Rodriguez FJ, et al. Photovoltaic/thermal solar hybrid system with bifacial PV module and transparent plane collector. Sol Energy Mat Sol C 2007;91(20):1966–71.
[11] Joge T, Eguchi Y, Imazu Y, Araki I, Uematsu T, Matsukuma K. Basic application technologies of bifacial photovoltaic solar modules. Electr Eng Jpn 2004;149(3):32–42.
[12] Nordmann T, Vontobel T, Clavadetscher L. 15 years of experience in construction and operation of two bifacial photovoltaic systems on Swiss roads and railways. In: Bifacial Workshop Konstanz 2012.
[13] Duffie JA, Beckman WA. Solar engineering of thermal processes. 2nd ed. New York: Wiley; 1991.
[14] Dimas FA, Gilani SI, Aris MS. Hourly solar radiation estimation from limited meteorological data to complete missing solar radiation data. In: International Conference on Environment Science and Engineering. Singapore 2011. p. 14–8.
[15] Liu BYH, Jordan RC. The interrelationship and characteristic distribution of direct, diffuse and total solar radiation. Sol Energy 1960;4(3):1–19.
[16] Campbell GS, Norman JM. Introduction to environmental biophysics. 2nd ed. New York: Springer; 1998.
[17] Celik AN. Long-term energy output estimation for photovoltaic energy systems using synthetic solar irradiation data. Energy 2003;28(5):479–93.
[18] Batlles FJ, Rubio MA, Tovar J, Olmo FJ, Alados-Arboledas L. Empirical modeling of hourly direct irradiance by means of hourly global irradiance. Energy 2000;25(7):675–88.
[19] Armstrong S, Hurley WG. A new methodology to optimise solar energy extraction under cloudy conditions. Renew Energy 2010;35(4):780–7.
[20] Wong LT, Chow WK. Solar radiation model. Appl Energy 2001;69(3):191–224.
[21] Reindl DT, Beckman WA, Duffie JA. Diffuse fraction correlations. Sol Energy 1990;45(1):1–7.
[22] Orgill JF, Hollands KGT. Correlation Equation for hourly diffuse radiation on a horizontal surface. Sol Energy 1977;19(4):357–9.
[23] Chieng YK, Green MA. Computer simulation of enhanced output from bifacial photovoltaic modules. Prog Photovolt Res Appl 1993;1(4):293–9.
[24] Dong R. Optimizing reflection and orientation for bifacial photovoltaic modules. The Ohio State University; 2009.
[25] Zhong H, Li GH, Tang RS, Dong WL. Optical performance of inclined south-north axis three-positions tracked solar panels. Energy 2011;36(2):1171–9.
[26] Li ZM, Liu XY, Tang RS. Optical performance of inclined south-north single-axis tracked solar panels. Energy 2010;35(6):2511–6.
[27] Martin N, Ruiz JM. Annual angular reflection losses in PV modules. Prog Photovolt 2005;13(1):75–84.
[28] Tian YQ, Davies-Colley RJ, Gong P, Thorrold BW. Estimating solar radiation on slopes of arbitrary aspect. Agr Forest Meteorol 2001;109(1):67–74.
[29] Kaldellis J, Zafirakis D. Experimental investigation of the optimum photovoltaic panels' tilt angle during the summer period. Energy 2012;38(1):305–14.
[30] Chang YP. Optimal the tilt angles for photovoltaic modules using PSO method with nonlinear time-varying evolution. Energy 2010;35(5):1954–63.
[31] Chang TP. Performance evaluation for solar collectors in Taiwan. Energy 2009;34(1):32–40.
[32] Gopinathan KK. Solar-radiation on variously oriented sloping surfaces. Sol Energy 1991;47(3):173–9.
[33] Shariah A, Al-Akhras MA, Al-Omari IA. Optimizing the tilt angle of solar collectors. Renew Energy 2002;26(4):587–98.
[34] Gunerhan H, Hepbasli A. Determination of the optimum tilt angle of solar collectors for building applications. Build Environ 2007;42(2):779–83.
[35] Surface meteorology and solar energyhttp://eosweb.larc.nasa.gov/sse/; 2013.
[36] ISLSCP II MODIS (COLLECTION 4) ALBEDO, 2002http://daac.ornl.gov/; 2013.
[37] NASA surface meteorology and solar energy: accuracyhttp://eosweb.larc.nasa.gov/cgi-bin/sse/sse.cgi?+s05#s05; 2013.
[38] Stroeve J, Box JE, Gao F, Liang SL, Nolin A, Schaaf C. Accuracy assessment of the MODIS 16-day albedo product for snow: comparisons with Greenland in situ measurements. Remote Sens Environ 2005;94(1):46–60.
[39] Privette JL, Zhang H, Mukelabai M, Schaaf CB. Characterization of MODIS land albedo (MOD43) accuracy with atmospheric conditions in Africa. Int Geosci Remote Sens 2004:4594–7.